Methyl and Ethyl Cation Affinities of Rare Gas Atoms and N_2

A. Cunje and A. C. Hopkinson*

Department of Chemistry, Centre for Research in Mass Spectrometry, York University, Toronto, Ontario, Canada M3J IP3

S. Yamabe*

Department of Chemistry, Nara University of Education, Takabatake-cho, Nara 630-8528, Japan

K. Hiraoka,* F. Nakagawa, M. Ishida, K. Fujita, K. Takao, A. Wada, and K. Hiizumi

Clean Energy Research Center, University of Yamanashi, Takeda-4, Kofu 400-8511, Japan

Received: February 13, 2004

Gas-phase methyl cation affinities (MCAs) for rare gases Ne, Kr, and Xe were measured with a pulsed electron-beam high-pressure mass spectrometer. The MCAs for Ne and Kr were determined to be 1.2 ± 0.3 and 19.8 ± 2.0 kcal/mol, respectively, by the observation of the clustering reaction, $CH_3^+ + Rg = CH_3^+(Rg)$ (Rg = Ne and Kr). The MCA of Xe was measured to be 2.0 ± 0.6 kcal/mol larger than that of N_2 by the observation of the substitution reaction $CH_3^+(N_2) + Xe = CH_3^+(Xe) + N_2$. Based on the MCA of N_2 of 44.1 kcal/mol proposed by McMahon et al., the MCA of Xe is determined to be 46.1 ± 0.6 kcal/mol. Molecular orbital calculations at six different levels consistently gave almost identical MCA values for each of the rare gases. At QCISD(T)(full)/6-311++G(2df,p)//B3LYP/6-311++G(d,p), the calculated values (all in kcal/mol) are as follows: He, 0.6; Ne, 2.2; Ar, 15.9; Kr, 24.1; and N_2, 43.2. For Xe at B3LYP/DZVP//B3LYP/DZVP, the calculated MCA is 39.0 kcal/mol. The ethyl cation affinities of Ar, Kr, and Xe were also measured. They are ~1.7, 3.2 ± 0.3, and 6.8 ± 0.3, respectively. The stabilities of $C_2H_5^+(Rg)$ and $C_2H_5^+(N_2)$ were discussed in terms of nonclassical (bridge) and classical (open) structures of $C_2H_5^+$.

1. Introduction

Carbocations play important roles in organic synthesis, combustion, organic plasmas, radiation chemistry, biology, chemical evolution in the interstellar space, and so forth. Because the methyl cation is the simplest carbocation and is one of the most reactive electrophilic agents, it has been extensively studied experimentally and theoretically. The methyl cation is the most electrophilic carbocation, while the rare gas atoms (Rg's) have closed shells and are basically inactive; for this reason, it is of fundamental interest to investigate the interactions between CH_3^+ and Rg atoms. McMahon et al. made a comprehensive study on the methyl cation affinities of a variety of compounds using a pulsed electron-beam high-pressure mass spectrometer and an ion cyclotron resonance mass spectrometer.[1,2] The MCAs determined by McMahon et al. for Kr and Xe were 39.7 and 46.6 kcal/mol, respectively, based on the MCA of N_2 (44.1 kcal/mol).[3,4,5a] Using the experimental proton affinities of neon and argon and extrapolating a plot of proton affinities versus methyl cation affinities, they also estimated the MCAs for Ne and Ar to be 26 and 36 kcal/mol, respectively.[1]

Hiraoka et al. measured the thermochemical stabilities of the cluster ions $CH_3^+(Ar)_n$ ($n = 1-8$) by observing the gas-phase equilibria for clustering reactions, $CH_3^+(Ar)_{n-1} + Ar = CH_3^+(Ar)_n$.[5b] The MCA for Ar was determined to be 11.3 kcal/mol, a value much lower than the MCA of Ar (36 kcal/mol) predicted by McMahon et al.[1] Heck et al. studied the translational energy-resolved collisionally activated methyl cation transfer from protonated methane to Ar, Kr, and Xe and from protonated fluoromethane to Ar and O_2.[6] They supported a value closer to that of McMahon et al. More recently, Dopfer et al., using IR photodissociation spectroscopic measurements, investigated the cluster ions of CH_3^+ with rare gas atoms.[7a,b,8a,b] The measured MCA of Ar (13 ± 4 kcal/mol)[8a] is in good agreement with that obtained by Hiraoka et al. (11.3 kcal/mol).[5b]

Gora and Roszak studied the molecular structures and nature of interactions in $CH_3^+(Ar)_n$ ($n = 1-8$) complexes theoretically.[9] Their theoretical dissociation energies for the cluster ions $CH_3^+(Ar)_n$ are in excellent agreement with experimental data of Dopfer et al.[8a] and Hiraoka et al.[5b] Geometries of some $CH_3^+(Rg)$ systems were examined theoretically.[5c,d]

In the present work, equilibria for the clustering reactions 1 and 2 and the exchange reaction 3 were studied in order to determine the MCAs for Ne, Kr, and Xe. Those reactions are defined in Table 1.

Molecular orbital calculations at several levels of theory have been used to calculate MCAs of He, Ne, Ar, Kr, Xe, and N_2, and these are compared with experimental values.

Ethyl cation, $C_2H_5^+$, has a nonclassical bridge structure.[10] Usually, hydrocarbons are composed of tight C−H covalent bonds, and transient C···H bonds are not permitted. On account of facile conversion of the nonclassical geometry to the classical one, equilibria in the clustering reactions, $C_2H_5^+(ligand)_{n-1} + ligand \leftrightarrows C_2H_5^+(ligand)_n$, are sometimes contaminated.[11] The contamination arises from the similar stability of classical $C_2H_5^+$-

* To whom correspondence should be addressed. E-mail: hiraoka@ab11.yamanashi.ac.jp.

10.1021/jp040133x CCC: $27.50
Published on Web 11/25/2004

TABLE 1: Experimental ($\Delta H°$ and $\Delta S°$) Thermochemical Data[a]

reaction		$-\Delta H°$	$-\Delta S°$
1	$CH_3^+ + Ne = CH_3^+(Ne)$	1.2 ± 0.3	18 ± 2
2	$CH_3^+ + Kr = CH_3^+(Kr)$	19.8 ± 2.0	26 ± 3
	$CH_3^+ + Ar = CH_3^+(Ar)$	11.3 ± 2.0[c]	26 ± 4[c]
3	$CH_3^+(N_2) + Xe = CH_3^+(Xe) + N_2$	2.0 ± 0.6	-3 ± 3
9	$C_2H_5^+ + Ar = C_2H_5^+(Ar)$	~ 1.7	~ 14
10	$C_2H_5^+ + Kr = C_2H_5^+(Kr)$	3.2 ± 0.3	22 ± 2
10	$C_2H_5^+(Kr) + Kr = C_2H_5^+(Kr)_2$	3.0 ± 0.5	23 ± 4
11	$C_2H_5^+ + Xe = C_2H_5^+(Xe)$	6.8 ± 0.3	21 ± 3
	$C_2H_5^+(Xe) + Xe = C_2H_5^+(Xe)_2$	~ 3.2	(18)[b]
12	$C_2H_5^+ + N_2 = C_2H_5^+(N_2)$	3.7 ± 0.3	16 ± 2
12	$C_2H_5^+(N_2) + N_2 = C_2H_5^+(N_2)_2$	3.5 ± 0.5	19 ± 4

[a] $\Delta H°$ is in kcal/mol and $\Delta S°$ is in cal/mol K (standard state, 1 atm). [b] Entropy value assumed. [c] Reference 5b.

(ligand) and nonclassical $C_2H_5^+$(ligand). It is tempting to measure thermochemical data of $C_2H_5^+(Rg)_1$ to infer the cluster geometry [$(H_2C-H-CH_2)^+\cdots Rg$ or $H_3C-H_2C^+\cdots Rg$]. When the $C_2H_5^+\cdots Rg$ interaction is weak, the nonclassical form of $C_2H_5^+$ is retained and the binding energies would increase gradually as Ne → Ar → Kr → Xe. When a sudden increase is observed, the geometrical change would be involved. In this work, gas-phase clustering reactions, $C_2H_5^+(Rg)_{n-1} + Rg \rightleftarrows C_2H_5^+(Rg)_n$, Rg = Ar, Kr, and Xe, were investigated for the inference. As a reference, reactions $C_2H_5^+(N_2)_{n-1} + N_2 \rightleftarrows C_2H_5^+(N_2)_n$ were also examined.

2. Experimental and Computational Methods

The experiments were carried out with a pulsed electron-beam high-pressure mass spectrometer.[12,13] For the observation of equilibria for reactions 1 and 2, about 3 Torr of the Rg major gas (Ne or Kr) was purified by passing it through a dry ice acetone-cooled 5 Å molecular sieve trap. The CH_3^+-forming reagent gas, CH_4, was introduced into the major gas through a flow-controlling stainless steel capillary. The CH_3^+ ion was formed from the charge-transfer reaction of Ne^+ with CH_4 with the rate constant of 1.7×10^{-11} cm^3 molecule^{-1} s^{-1}.[14]

$$Ne^+ + CH_4 \rightarrow CH_4^+ + Ne\ (52\%) \quad (4a)$$

$$\rightarrow CH_3^+ + H + Ne\ (24\%) \quad (4b)$$

$$\rightarrow CH_2^+ + H_2 + Ne\ (20\%) \quad (4c)$$

$$\rightarrow CH^+ + H_2 + H + Ne\ (4\%) \quad (4d)$$

In the charge-transfer reaction of Kr^+ with CH_4, the CH_3^+ ion was produced at the collision rate ($1.2 \pm 0.05 \times 10^{-9}$ cm^3 molecule^{-1} s^{-1}).[15]

$$Kr^+ + CH_4 \rightarrow CH_3^+ + H + Kr\ (35\%) \quad (5a)$$

$$\rightarrow CH_4^+ + Kr\ (65\%) \quad (5b)$$

The partial pressure of CH_4 was kept lower than 10 μTorr, to prevent the rapid decay of the CH_3^+ ion by reaction 6.

$$CH_3^+ + CH_4 \rightarrow C_2H_5^+ + H_2 \quad (6)$$

Due to the low partial pressure of the reagent gas CH_4, the concentration of CH_3^+ was small and special care had to be taken in the measurement for equilibria of reactions 1 and 2 for the precise measurement.

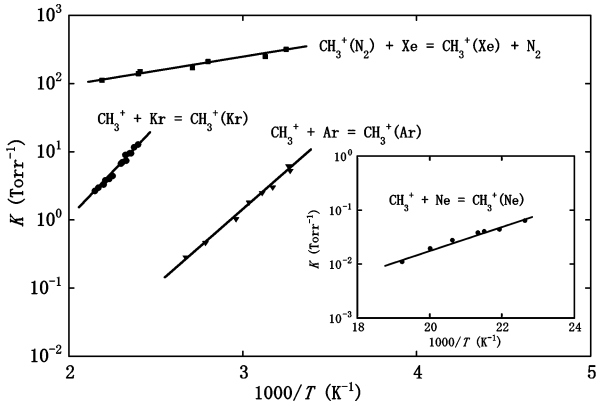

Figure 1. van't Hoff plots for clustering reactions (1) $CH_3^+ + Ne = CH_3^+(Ne)$, $CH_3^+ + Ar = CH_3^+(Ar)$; and (2) $CH_3^+ + Kr = CH_3^+(Kr)$; and for exchange reaction (3) $CH_3^+(N_2) + Xe = CH_3^+(Xe) + N_2$.

For the measurement of equilibria for exchange reaction 3, about 3 Torr of the major gas N_2 was purified by passing it through a dry ice acetone-cooled 5 Å molecular sieve trap. The reagent gas Xe of 100−500 mTorr and the CH_3^+-forming CH_4 gas with pressure less than 10 μTorr were introduced into the major gas N_2 through flow-controlling stainless steel capillaries.

Molecular orbital calculations were performed using Gaussian 98.[16] Structure optimizations were carried out at three different levels of theory. First, density functional theory (DFT) with Becke's three-parameter hybrid functional[17,18] and the LYP correlation functional[19] (B3LYP) along with the double-ζ split-valence + polarization basis set DZVP[20] was used for optimizations on all the ions. All stationary points were characterized by harmonic frequency calculations and were found to be at minima. As a check on the accuracy of the results obtained using the DZVP basis set, second, optimizations were performed at B3LYP/6-311++G(d,p) and at MP2(full)/6-311++G(d,p)[21] on all ions except CH_3^+(Xe). To improve energies, single-point calculations were performed at QCISD(T)(full)/6-311++G-(2df,p)//B3LYP/6-311++G(d,p), at MP4SDTQ(full)6-311++G-(2df,p)/MP2(full)/6-311++G(d,p), and at G2MP2. Because of the error bars (11.3 ± 2[5b] and 13 ± 4[8a] kcal/mol) in the experimental values for the methyl cation affinity of argon, we subjected this ion to a third optimization at an even higher level, CCSD(T)(full)/6-311++G(3df,3pd).

3. Results and Discussion

(a) Experimental Assessment of Methyl Cation Affinities. Figure 1 shows the van't Hoff plots for clustering reactions 1 and 2 together with that for Ar.[5b] The measurements for the higher order clustering reactions of CH_3^+ with Kr were made difficult by the presence of the isotopes of Kr (i.e., 80(2.2%), 82(11.6%), 84 (57%), and 86(17%)). As the temperature was decreased, cluster ions $CH_3^+(Kr)_n$ were contaminated by ions $CH_4^+(Kr)_n$ and also $CH_5^+(Kr)_n$. Consequently, no reliable equilibrium constants for higher order clustering reactions could be measured. The thermochemical data obtained are summarized in Table 1. The obtained bond energy for $CH_3^+\cdots Kr$ (19.8 ± 2.0 kcal/mol) is much smaller than that (39.7 kcal/mol) obtained by McMahon et al.[4] Such a large discrepancy is difficult to explain because the data were obtained by similar experimental techniques, i.e., the gas-phase equilibrium measurement. Hovey and McMahon determined the relative MCAs of Kr and N_2 by observing the equilibria for exchange reaction 7 using an ion

TABLE 2: Methyl Cation Affinities (kcal/mol) from Molecular Orbital Calculations and Experiments

	B3LYP[a]	QCI	MP2	MP4	B3LYP[b]	G2MP2	expt (this work)	expt (lit)
He	1.7	0.6	0.5	0.9	1.0	1.1		
Ne	2.2	2.5	1.3	2.3	3.0	2.5	1.2	
Ar[c]	15.0	15.8	13.9	16.3	14.4	17.2		11.3 ± 2[d]
								13 ± 4[e]
Kr	24.5	24.2	21.5	25.0	24.2	25.5	19.8	44.5[f]
Xe					39.0		46.1	51.5 ± 3[f]
N_2	42.7	43.2	43.2	44.2	45.0	43.2		44.1[g]

[a] B3LYP/6-311++G(d,p). [b] B3LYP/DZVp. [c] At CCSD(T)(full)/6-311++G(3df,3pd), the calculated MCA for Ar is 16.4 kcal/mol. [d] Reference 5b. [e] Reference 8a. [f] Reference 1. [g] Reference 4.

cyclotron resonance (ICR) mass spectrometer (see Figure 3 in ref 1).

$$CH_3^+(Kr) + N_2 = CH_3^+(N_2) + Kr \qquad (7)$$

They confirmed that the measured equilibrium constants were independent of the ratio [Kr]/[N_2], varying values from 7:1 to 20:1 at 298 K, and concluded that the MCA of Kr is 4.4 kcal/mol smaller than that of N_2. To reproduce their measurements, we introduced 1 mTorr of N_2 into the 4 Torr Kr major gas containing about 10 μTorr of CH_4 at 298 K. It was found that the primary CH_3^+(Kr) ion was completely converted to CH_3^+-(N_2) within 0.1 ms. This indicates that the MCA of Kr is much smaller than that of N_2. Again, a serious discrepancy was found between the Hovey/McMahon experiment (ICR measurement)[1] and the present work (high-pressure mass spectrometer measurement). One possibility for the discrepancy is that the equilibrium for reaction 7 was not established in the Hovey/McMahon experiments, but they confirmed the establishment of the equilibria for the reaction. At present, we do not understand why different behavior is observed by different experimental instruments. Two MCA values will be assessed by the calculated energies in the next subsection.

We attempted to determine the MCA of Xe directly by observing the equilibrium for reaction 8.

$$CH_3^+ + Xe = CH_3^+(Xe) \qquad (8)$$

However, equilibrium could not be established with the ion source temperature up to 730 K. This indicates that the enthalpy change ($-\Delta H°$) for reaction 8 (i.e., MCA of Xe) is much higher than ~30 kcal/mol. To determine the MCA of Xe relative to that of N_2, the van't Hoff plots for equilibria of the exchange reaction 3 were measured and are shown in Figure 1. The obtained thermochemical data, $\Delta H°$ (-2.0 ± 0.6 kcal/mol) and $\Delta S°$ (3 ± 3 cal/mol K), are in good agreement with $\Delta H°$ (-2.5 kcal/mol) and $\Delta S°$ (7.8 cal/mol K) determined by McMahon et al.[2] using a high-pressure mass spectrometer. Thus, it can unequivocally be concluded that the MCA of Xe is 2.0−2.5 kcal/mol larger than that of N_2. The experimental MCAs for rare gases and N_2 are summarized in the right side of Table 2.

(b) Computational Assessment of Methyl Cation Affinities. The calculated MCAs listed in Table 2 are much smaller than the proton affinities (PAs) in Table S1 (Supporting Information). For each rare gas atom, the various levels of theory give similar values and, unlike in the calculation of PAs, the B3LYP/DZVP values are in good agreement with those from other levels of theory. For N_2, the standard used to anchor other MCAs,[4] theory values range from 42.7 to 45.0 kcal/mol. For He and Ne, the MCAs are very small. The nonrigidity in He−CH_3^+ and Ne−CH_3^+ complexes was examined in detail.[7a,b,8b] The complexes have long Rg−CH_3^+ bonds (where Rg is He or Ne) (see Table S2, Supporting Information) and consequently these ions are probably not very well described by molecular orbital theory. Nevertheless, the calculations give an MCA in the range 1.3−3.0 kcal/mol for Ne, slightly higher than our measured value of 1.2 ± 0.3 kcal/mol.

Neon and carbon atoms belong to the second row, and the $CH_3^+ \leftarrow$ Ne charge transfer (CT) might be large owing to the effective overlap of 2p orbitals. However, the methyl cation has pair electrons of three C−H bonds, which undergo large exchange repulsion against Ne p_π electrons. The repulsion results in the unexpectedly small CT and CH_3^+···Ne bonding energy.[7b,8b]

For Ar, for which two slightly different MCAs are quoted in the literature,[1,5b,8a,9] theory gives values in the range 13.9−17.2 kcal/mol and the average over seven calculated values is 15.6 kcal/mol. The highest level calculation, a full optimization at CCSD(T)(full)/6-311++G(3df,3pd), gave an MCA of 16.4 kcal/mol. Counterpoise calculations correcting for basis set superposition errors (BSSE) made essentially no difference to the numbers in Table 2;[22,23] BSSE corrections have the effect of reducing binding energies, so any minor correction would *reduce* the calculated MCA. We therefore conclude that the experimental value of 11.3 ± 2 kcal/mol is more reliable than the value of 37.4 kcal/mol obtained by extrapolating the MCA/PA plot.[2]

For Kr, the calculated values are in the range 21.5−25.5 kcal/mol (the average over six values is 24.2 kcal/mol). Indeed, these are all slightly higher than our experimental value of 19.8 ± 2.0 kcal/mol, but they support it rather than the previous value (44.5 kcal mol^{-1}).[1]

The computational result for Xe is more difficult to reproduce where we have only one level of theory (B3LYP/DZVP) due to unavailability of basis sets. Experimentally, methyl cation transfer from CH_3^+(N_2) to Xe is exothermic by 2.0 ± 0.6 kcal/mol, while theory gives it to be endothermic by 6 kcal/mol. Assuming that the calculations on N_2 are reliable (the average calculated value of 43.6 kcal/mol compares with the experimental value of 44.1 kcal/mol), then the discrepancy between experiment and theory for CH_3^+ transfer between N_2 and Xe is most likely to be in the calculation of the MCA of Xe.[24]

All the methyl adducts of rare gases, CH_3^+(Rg), have C_{3v} symmetry, and the distortion of the RgCH angle from 90° correlates roughly with the MCA of Rg.[5a,c,d] Both He and Ne interact very weakly with CH_3^+, and angle RgCH is close to 90° (see Table S2 in the Supporting Information). When Rg is Ar, Kr, and Xe, angle RgCH is slightly greater than 100° and in CH_3^+(N_2) it is 106.0°.

(c) Experimental Assessment of Ethyl Cation Affinities. When a H atom in CH_3^+ is substituted by the methyl group (i.e., $CH_3^+ \rightarrow C_2H_5^+$), the reactivity would be greatly reduced due to the hyperconjugative effect of methyl. In this respect, the measurement of ethyl cation affinities of rare gases and also N_2 would give a measure of the hyperconjugation relative to MCAs. The van't Hoff plots for clustering reactions 9−12 are shown in Figure 2. Those reactions are defined in Table 1.

For reactions 10−12, sound equilibria were observed in all the temperature range measured. However, the equilibria for reaction 9 were found not to be observed below ~95 K ($1000/T \geq \sim 10.6$). It was found that the decay rate of $C_2H_5^+$(Ar) became slower than that of $C_2H_5^+$ below ~95 K and measured apparent equilibrium constants deviate downward from the extrapolated van't Hoff plots in Figure 2. This is probably due to the

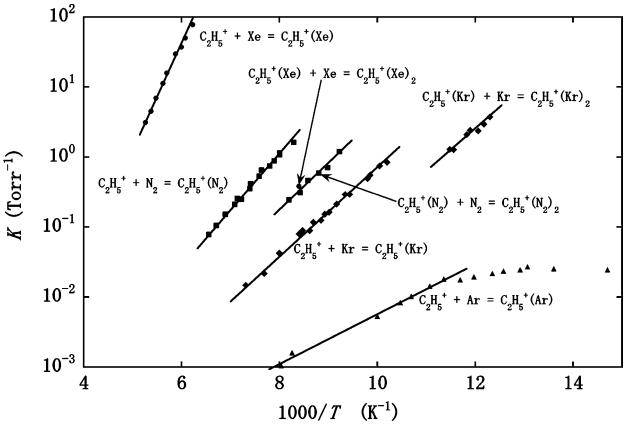

Figure 2. van't Hoff plots for clustering reactions (9) $C_2H_5^+ + Ar = C_2H_5^+(Ar)$, (10) $C_2H_5^+(Kr)_{n-1} + Kr = C_2H_5^+(Kr)_n$, (11) $C_2H_5^+(Xe)_{n-1} + Xe = C_2H_5^+(Xe)_n$, and (12) $C_2H_5^+(N_2)_{n-1} + N_2 = C_2H_5^+(N_2)_n$.

existence of some impurities. Thus, the thermochemical data for reaction 9 in Table 1 are only approximate ones.

The ethyl cation affinities (ECAs) of Ar, Kr, Xe, and N_2 were measured to be ~1.7, 3.2 ± 0.3, 6.8 ± 0.3, and 3.7 ± 0.3 kcal/mol, respectively. The measured ECAs are much smaller than MCAs (Tables 1 and 2). Apparently, unlike in the interaction between the methyl cation and Rg atoms, the ethyl cation does not form strong covalent bonds with Rg atoms or N_2. In our previous work, theoretical calculations predicted that the gas-phase $C_2H_5^+$ ion has only the nonclassical bridged structure and the isomer with the classical structure is a transition state for H-exchange.[11] It was also predicted that the nonclassical bridged structure $C_2H_5^+$ isomerizes to the classical one when the $C_2H_5^+$ ion binds with CH_4 to form the cluster ion $C_2H_5^+\cdots CH_4$.[25] The bond energy for $C_2H_5^+\cdots CH_4$ was measured to be 5.5 kcal/mol.

$$C_2H_5^+(CH_4)_{n-1} + CH_4 = C_2H_5^+(CH_4)_n \qquad (13)$$

The cluster ion $C_2H_5^+\cdots CH_4$ is the C−C bond protonated propane; that is, the cluster ion has some covalent character and the positive charge in $C_2H_5^+$ is more or less dispersed in $C_2H_5^+\cdots CH_4$. In fact, the enthalpy changes $-\Delta H^\circ_{n-1,n}$ show a sharp decrease from $n = 1$ (5.5 kcal/mol) to $n = 2$ (2.4 kcal/mol). The decrease suggests that there are some bonding changes with $n = 1 \rightarrow 2$ in the cluster ion $C_2H_5^+(CH_4)_n$. In Figure 2, the van't Hoff plots for reaction 10 with $n = 1$ and 2 are quite close to each other and the values of $-\Delta H^\circ_{n-1,n}$ are nearly *n*-independent (3.2 ± 0.3 kcal/mol for $n = 1$ and 3.0 ± 0.5 kcal/mol for $n = 2$). This indicates that the $C_2H_5^+$ ion and Kr atoms interact only weakly with the electrostatic interaction. In contrast, there is a large gap between the van't Hoff plots between $n = 1$ and 2 for reaction 11 in Figure 2 (only a single measurement with $n = 2$ was possible at a temperature just above the condensation point of the reagent gas Xe in Figure 2). This suggests that a weak coordination bond is formed in the complex $C_2H_5^+\cdots Xe$ and the nature of bonding changes from coordination bonding for $n = 1$ to electrostatic for larger cluster ions ($n \geq 2$). The cluster ion $C_2H_5^+(Xe)_n$ may be represented as the core ion $[C_2H_5\cdots Xe]^+$ with surrounding Xe ligands, $[C_2H_5\cdots Xe]^+(Xe)_{n-1}$.

In Table 1, the ECA of N_2 (3.7 ± 0.3 kcal/mol) is smaller than that of Xe (6.8 ± 0.3 kcal/mol) and the values of $-\Delta H^\circ_{n-1,n}$ for reaction 12 are nearly *n*-independent for $n = 1$ and 2. This indicates that the $C_2H_5^+$ ion interacts with N_2 molecules electrostatically. This is in contrast to the fact that the complex $C_2H_5^+\cdots Xe$ has some coordination bond character. Apparently, the Xe atom is more polarizable than the N_2 molecule. This is in line with the fact that the MCA for Xe is larger than that for N_2. The decisively different MCA and ECA for N_2 suggest that the $CH_3^+N_2$ geometry is entirely different from the $C_2H_5^+N_2$ one.

TABLE 3: Calculated Enthalpies and Entropies (at 298 K) for Complexes Containing the Ethyl Cation as Calculated at B3LYP/DZVP[a]

reaction		$-\Delta H^\circ$	$-\Delta S^\circ$
9	$C_2H_5^+ + Ar = C_2H_5^+(Ar)$	1.2	16.8
10	$C_2H_5^+ + Kr = C_2H_5^+(Kr)$	3.3	22.7
10	$C_2H_5^+(Kr) + Kr = C_2H_5^+(Kr)_2$	1.3	16.8
11	$C_2H_5^+ + Xe = C_2H_5^+(Xe)$	8.2	23.7

[a] ΔH° is in kcal/mol and ΔS° is in cal/mol K (standard state, 1 atm).

CHART 1: Geometric Patterns of $C_2H_5^+(R_g)_n$ ($n = 1$ and 2) and $C_2H_5^+(N_2)_1$

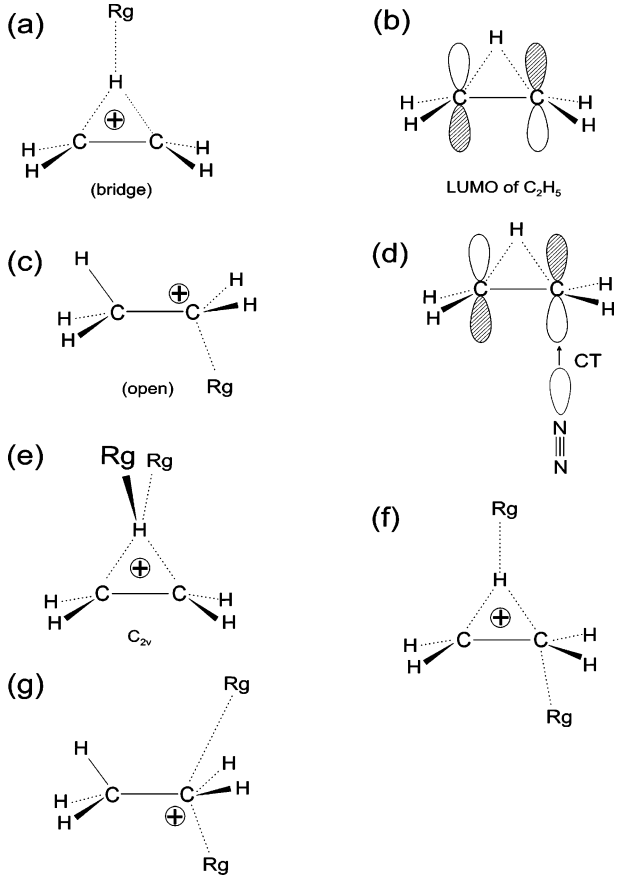

(d) Computational Assessment of Ethyl Cation Affinities. Calculated values for reactions 10 ($n = 1$ and 2) and for reaction 11 ($n = 1$) are given in Table 3. The calculated enthalpies agree moderately well with the experimental values in Table 1. In the previous subsection, the geometries of $C_2H_5^+(Rg)_n$ and $C_2H_5^+(N_2)_n$ were conjectured in consideration of the enthalpy changes. Basically, there are two isomers of $C_2H_5^+(Rg)_1$ (Rg = Ar, Kr, and Xe) and $C_2H_5^+(N_2)_1$, which are shown as panels a and c in Chart 1. In general, isomer c is more stable in ΔH° but less stable in $-T\Delta S^\circ$ of ΔG° than isomer a. $C_2H_5^+(Ar)_1$ and $C_2H_5^+(Kr)_1$ were computed to be of isomer a in Gibbs free energies. The top Ar···H and Kr···H distances are 2.52 and 2.59 Å, respectively. In contrast, for $C_2H_5^+(N_2)_1$, isomer c is 2.03 kcal/mol more stable (free energies) than isomer a. However, the $C_2H_5^+$(open)···N_2 bonding energy, 7.65 kcal/mol, is unreasonably larger than the present experimental one, 3.7 ± 0.3 kcal/mol, and the $C_2H_5^+$(bridge)···N_2 calculated one, 3.19 kcal/mol. The open isomer $C_2H_5^+(N_2)_1$ would be prohibitive owing to

the strict directionality at the $N_2 \rightarrow C_2H_5^+$ coordination. In Chart 1b, the lowest unoccupied molecular orbital (LUMO) of $C_2H_5^+$ is shown. The LUMO is of antisymmetric orbital phase, with which the N_2 bond axis must be aligned strictly to afford isomer c as shown in Chart 1d. The strict orientation is not required for the hydrogen-bond-type coordination in isomer a.

As the Rg atoms get larger, Ar → Kr → Xe, the ionization potential becomes smaller, 15.8 → 14.0 → 12.1 eV, and accordingly CT is stronger. The strong CT in $C_2H_5^+(Xe)_1$ might make isomer c more stable than isomer a. In fact, the former is 4.51 kcal/mol more stable in free energies. In addition, the large-size and spherical valence orbitals of Xe may donate electronic charges to the LUMO of $C_2H_5^+$ without difficulty of the strict directionality.

For $C_2H_5^+(Kr)_2$ and $C_2H_5^+(N_2)_2$, there are two isomers, panels e and f in Chart 1. Isomer f was calculated to be more stable, where the bridge form is somewhat distorted but is retained. The C···Kr distance, 3.285 Å, in isomer f ($n = 2$) is much larger than that (2.582 Å) in isomer c ($n = 1$). The C···Kr and C···N_2 interaction in isomer f ($n = 2$) is not of CT but of the long-range van der Waals type. In Table 1, $\Delta H°_{n-1,n}$ and $\Delta S°_{n-1,n}$ for $C_2H_5^+(Kr)_n$ and $C_2H_5^+(N_2)_n$ show anomalous changes. The result of $-\Delta H°_{0,1} = 3.7 \pm 0.3$ kcal/mol $> -\Delta H°_{1,2} = 3.5 \pm 0.5$ kcal/mol for $C_2H_5^+(N_2)_n$ should give that of $-\Delta S°_{0,1} > -\Delta S°_{1,2}$. But the experimental result is the opposite, $-\Delta S°_{1,2} = 16 \pm 2$ eu $< -\Delta S°_{1,2} = 19 \pm 4$ eu. The apparent anomaly may be explicable by the different N_2 coordinations to $C_2H_5^+$, $N_2\cdots HC_2H_4^+$ and $N_2\cdots CH_2HCH_2^+$, in $n = 2$. The $C_2H_5^+(Xe)_2$ cluster was computed to have the shape of isomer g in Chart 1. The two Xe···C distances are 2.632 and 3.546 Å, respectively, which explains the large falloff, 6.8 ± 0.3 kcal/mol → ∼3.2 kcal/mol in Table 1. Those B3LYP/DZP results are confirmed to be similar to those of MP2/DZP.

4. Concluding Remarks

Gas-phase affinities of methyl and ethyl cations (MCA and ECA) for rare gas atoms and N_2 have been measured with a pulsed electron-beam high-pressure mass spectrometer. MCA values for Ar, Xe, and Ne are in good agreement with the previous experimental and the present computational data. The MCA value for Kr (=19.8 kcal/mol) is, however, much smaller than the precedent, 44.5 kcal/mol, and is somewhat smaller than the present calculated one, ∼24 kcal/mol.

ECA values have been obtained for the first time. The ECA for Ar is very small (∼1.7 kcal/mol), which suggests that Ar is in contact not with the ethyl carbon of $C_2H_5^+$ but with the bridge hydrogen. The coordination has been found by the calculations and has been obtained also for $C_2H_5^+(Kr)_1$ and $C_2H_5^+(N_2)_1$. The ECA for Kr (=3.2 ± 0.3 kcal/mol) is close to the ECA for N_2 (=3.7 ± 0.3 kcal/mol). The second Kr and N_2 are bound to $C_2H_5^+(Kr)_1$ and $C_2H_5^+(N_2)_1$, respectively, with similar stabilizing energies, ∼3 kcal/mol, but with different coordinations. The largest ECA (=6.8 ± 0.3 kcal/mol) has been obtained for Xe, where the ethyl cation has an open (classical) form. The second Xe is bound weakly to $C_2H_5^+(Xe)_1$. The extent of the falloff, $-\Delta H°_{0,1} \rightarrow -\Delta H°_{1,2}$, seems to be related to a diagnosis of nonclassical or classical form of $C_2H_5^+$. Since the basis set of Xe used here is of moderate size and the present B3LYP/DZP calculated results would not be definitive, geometric discussions need to be regarded as qualitative ones.

Supporting Information Available: The calculated proton affinities of Rg's and N_2 (Table S1). Geometries of the protonated Rg's and N_2, $CH_3^+(Rg)$ and $CH_3^+(N_2)$ (Table S2). This material is available free of charge via the Internet at http://pubs.acs.org.

References and Notes

(1) Hovey, J. K.; McMahon, T. B. *J. Phys. Chem.* **1987**, *91*, 4560.

(2) McMahon, T. B.; Heinis, T.; Nicol, G.; Hovey, J. K.; Kebarle, P. *J. Am. Chem. Soc.* **1988**, *110*, 7591.

(3) Foster, M. S.; Williamson, A. D.; Beauchamp, J. L. *Int. J. Mass Spectrom. Ion Phys.* **1974**, *15*, 429.

(4) Glukhovtsev, M. N.; Szulejko, J. E.; McMahon, T. B.; Gauld, J. W.; Scott, A. P.; Smith, B. J.; Pross, A.; Radom, L. *J. Phys. Chem.* **1994**, *98*, 13099.

(5) (a) Hiraoka, K.; Takao, K.; Nakagawa, F.; Iino, T.; Ishida, M.; Fujita, K.; Hiizumi, K.; Yamabe, S. *Int. J. Mass Spectrom.* **2003**, *227*, 391. (b) Hiraoka, K.; Kudaka, I.; Yamabe, S. *Chem. Phys. Lett.* **1991**, *178*, 103. (c) Cunje, A.; Rodriquez, C. F.; Bohme, D. K.; Hopkinson, A. C. *Can. J. Chem./Rev. Can. Chim.* **1998**, *76*, 1138. (d) Cunje, A.; Rodriquez, C. F.; Bohme, D. K.; Hopkinson, A. C. *J. Phys. Chem. A* **1998**, *102*, 478.

(6) Heck, A. J. R.; de Koning, L. J.; Nibbering, N. M. M. *J. Phys. Chem.* **1992**, *96*, 8870.

(7) (a) Olkhov, R. V.; Nizkorodov, S. A.; Dopfer, O. *J. Chem. Phys.* **1999**, *110*, 9527. (b) Dopfer, O.; Olkov, R. V.; Maier, J. P. *J. Chem. Phys.* **2000**, *112*, 2176.

(8) (a) Olkhov, R. V.; Nizkorodov, S. A.; Dopfer, O. *J. Chem. Phys.* **1998**, *108*, 10046. (b) Dopfer, O.; Luckhaus, D. *J. Chem. Phys.* **2002**, *116*, 1012. (c) Dopfer, O. *Int. Rev. Phys. Chem.* **2003**, *22*, 437.

(9) Gora, R. W.; Roszak, S. *J. Chem. Phys.* **2001**, *115*, 771.

(10) (a) Koeler, H.-J.; Lischka, H. *Chem. Phys. Lett.* **1978**, *58*, 175. (b) Hirao, K.; Yamabe, S. *Chem. Phys.* **1984**, *89*, 237. (c) Dewar, M. J. S.; Ford, G. P. *J. Am. Chem. Soc.* **1979**, *101*, 783. (d) Ruo-Zhuang, L.; Jian-Guo, Y. *Int. J. Quantum Chem.* **1983**, *23*, 491. (e) Ruscic, B.; Berkowitz, J.; Curtiss, L. A.; Pople, J. A. *J. Chem. Phys.* **1989**, *91*, 114. (f) Klopper, W.; Kutzelnigg, W. *J. Phys. Chem.* **1990**, *94*, 5625. (g) Obata, S.; Hirao, K. *Bull. Chem. Soc. Jpn.* **1993**, *66*, 3271. (h) Perera, S. A.; Bartlett, R. J.; Schleyer, P. v. R. *J. Am. Chem. Soc.* **1995**, *117*, 8476. (i) Lammertsma, K.; Ohwada, T. *J. Am. Chem. Soc.* **1996**, *118*, 7247.

(11) Hiraoka, K.; Shoda, T.; Kudaka, I.; Fujimaki, S.; Mizuse, S.; Yamabe, S.; Wasada, H.; Wasada-Tsutui, Y. *J. Phys. Chem. A* **2003**, *107*, 775.

(12) Kebarle, P. In *Technique for the Study of Ion−Molecule Reactions*; Farrar, J. M., Saunders, W. H., Jr., Eds.; Wiley: New York, 1971; p 221.

(13) Hiraoka, K.; Yamabe, S. In *Dynamics of Excited Molecules*; Kuchitsu, K., Ed.; Elsevier: Amsterdam, 1994; p 399.

(14) Rakshit, A. B.; Twiddy, N. D. *Chem. Phys. Lett.* **1979**, *60*, 400.

(15) Li, Y.-H.; Harrison, A. G. *Int. J. Mass Spectrom. Ion Phys.* **1978**, *28*, 289.

(16) Frisch, M. J.; Trucks, G. W.; Schlegel, H. B.; Scuseria, G. E.; Robb, M. A.; Cheeseman, J. R.; Zakrzewski, V. G.; Montgomery, J. A., Jr.; Stratmann, R. E.; Burant, J. C.; Dapprich, S.; Millam, J. M.; Daniels, A. D.; Kudin, K. N.; Strain, M. C.; Farkas, O.; Tomasi, J.; Barone, V.; Cossi, M.; Cammi, R.; Mennucci, B.; Pomelli, C.; Adamo, C.; Clifford, S.; Ochterski, J.; Petersson, G. A.; Ayala, P. Y.; Cui, Q.; Morokuma, K.; Malick, D. K.; Rabuck, A. D.; Raghavachari, K.; Foresman, J. B.; Cioslowski, J.; Ortiz, J. V.; Stefanov, B. B.; Liu, G.; Liashenko, A.; Piskorz, P.; Komaromi, I.; Gomperts, R.; Martin, R. L.; Fox, D. J.; Keith, T.; Al-Laham, M. A.; Peng, C. Y.; Nanayakkara, A.; Gonzalez, C.; Challacombe, M.; Gill, P. M. W.; Johnson, B. G.; Chen, W.; Wong, M. W.; Andres, J. L.; Head-Gordon, M.; Replogle, E. S.; Pople, J. A. *Gaussian 98*, revision A.7; Gaussian, Inc.: Pittsburgh, PA, 1998.

(17) Becke, A. D. *Phys. Rev. A* **1988**, *38*, 3098.

(18) Becke, A. D. *J. Chem. Phys.* **1993**, *93*, 5648.

(19) Lee, C.; Yang, W.; Parr, R. G. *Phys. Rev. B* **1988**, *37*, 785.

(20) Basis sets were obtained from the Extensible Computational Chemistry Environment Basis Set Database, Version 1.0, as developed and distributed by the Molecular Science Computing Facility, Environmental and Molecular Sciences Laboratory, which is part of the Pacific Northwest Laboratory, P.O. Box 999, Richland, WA 99352, and funded by the U.S. Department of Energy. The Pacific Northwest Laboratory is a multiprogram laboratory operated by Battelle Memorial Institute for the U.S. Department of Energy under Contract DE-AC06-76RLO 1830.

(21) Møller, C.; Plesset, M. S. *Phys. Rev.* **1984**, *46*, 618.

(22) Boys, S. F.; Bernardi, F. *Mol. Phys.* **1991**, *95*, 4378.

(23) van Duijneveldt, F. B.; van Duijneveldt-van de Rijdt, J. G. C. M.; van Levithe, J. H. *Chem. Rev.* **1994**, *94*, 1873.

(24) The valence electronic configuration of Xe is $4f^05s^25p^6$. There is an inner vacant orbital, $4f^0$. This orbital is a strong electronic charge acceptor. For $CH_3^+(Xe)$, the 4f orbital of Xe should work in the back charge transfer (CT), $CH_3^+ \rightarrow Xe$. But, unfortunately, the inner vacant orbital cannot be described in molecular orbital calculations. Thus, disagreement of the Xe MCA in Table 2 comes from the lack of the back-CT, $CH_3^+ \rightarrow Xe$, in calculations. For the protonated Xe, there is no $H^+ \rightarrow Xe$ back CT and a good agreement has been obtained in Table S1 (Supporting Information).

(25) Hiraoka, K.; Mori, T.; Yamabe, S. *Chem. Phys. Lett.* **1993**, *207*, 178.